Desalination and Water Treatment
www.deswater.com

doi: 10.5004/dwt.2023.29727

300 (2023) 75–83
July

Exploring the kinetics, thermodynamics, and isotherms of sodium naproxen uptake by oak-based activated carbon with ultrasonic enhancement

Alaa M. Al-Ma'abreh[a,*], Manal AlKhabbas[a], Gada Edris[a], Mike Kh. Haddad[b], Dareen A Hmedat[a], Razan Ataallah Abuassaf[a], Samer Hasan Hussein-Al-Ali[a], Samer Alawaideh[a], Abdelmajeed Adam Lagum[c,*]

[a]*Department of Chemistry, Faculty of Science, Isra University, P.O. Box: 22, Amman 11622, Jordan, Tel.: +962-799011634/ +962-790857347; emails: alaa.almaabreh@iu.edu.jo/alaamabreh@yahoo.com (A.M. Al-Ma'abreh), Manal.khabbas@iu.edu.jo (M. AlKhabbas), Gadaedris@yahoo.com (G. Edris), Dareenhmedat@yahoo.com (D.A. Hmedat), razan.abuassaf@iu.edu.jo (R.A. Abuassaf), samer.alali@iu.edu.jo (S.H. Hussein-Al-Ali), Samerawaideh@yahoo.com (S. Alawaideh)*
[b]*Department of Renewable Energy Engineering, Faculty of Engineering, Isra University, P.O. Box: 22, Amman 11622, Jordan, email: mhaddad@iu.edu.jo (M. Kh. Haddad)*
[c]*Department of Civil Engineering, Faculty of Engineering, Isra University, Amman, Jordan, email: abdelmajeed.lagum@iu.edu.jo (A.A. Lagum)*

Received 9 February 2023; Accepted 20 June 2023

ABSTRACT

The efficacy of ultrasonic technology for the uptake of sodium naproxen (SN) onto oak-based activated carbon (OAC) was examined in this study. SN is a widely used medication around the globe. The investigation of the uptake of SN by OAC involved the analysis of Fourier-transform infrared spectroscopy, X-ray diffraction, and scanning electron microscopy techniques. The rate of SN uptake by OAC followed the pseudo-second-order kinetic model with a rate constant of 2.78×10^{-2} g·mg^{-1}·min^{-1}. A multilayer uptake of 94.8% was found by Freundlich isotherm. The thermodynamic analysis indicated that the adsorption of SN onto OAC was endothermic in nature with $\Delta H°$ value of 10.88 kJ·mol^{-1}. Additionally, OAC was observed to be reusable for up to six regeneration cycles with a minimal decline of 26.43% in its adsorption capacity compared to the initial performance using sodium hydroxide as an eluent. Undoubtedly, the ultrasonic technique demonstrated remarkable efficiency in enhancing the uptake of SN by OAC.

Keywords: Activated carbon; Adsorption; Oak; Sodium naproxen; Ultrasonic

1. Introduction

Pharmaceuticals that have a wide range of chemical structures are now recognized as a distinct category of environmental pollutants because of their widespread use and increasing utilization in human medicine. Among the most frequently reported pharmaceuticals in aquatic environments include beta-blockers, nonsteroidal anti-inflammatory drugs, antibiotics, lipid metabolism regulators, and antiepileptic drugs [1]. The most prescribed medications are analgesics. Among these analgesics is sodium naproxen (Fig. 1) which is also an anti-inflammatory that belongs to the nonsteroidal aryl acetic acid group. Sodium naproxen was found to be associated with water contamination. It can persist and accumulate in water bodies after entering through numerous means such as wastewater discharge or incorrect disposal. This accumulation can result in higher levels of drugs in water, potentially harmful water quality, and posing a risk to aquatic organisms and human health if the water is utilized for drinking or irrigation [2].

* Corresponding authors.

Different approaches for reducing pharmaceutical micropollutants from contaminated water were developed. Pollutants are usually removed from water by physical and chemical methods. Chemical water purification methods include disinfection, desalination, coagulation, and precipitation [3]. Bio- and photo-degradation are additional methods for reducing pollutants such as dyes [4]. Adsorption is a frequently used approach for reducing contaminants in water because of its high efficacy, low toxicity, simplicity, non-destructiveness, and insignificant cost [5]. One of the most used materials as an adsorbent is activated carbon because of its unique properties such as high surface area, high degree of porosity, and distinctive chemical properties that support the interaction with numerous chemical substances [6]. It is feasible to make activated carbon from a variety of carbonaceous materials, such as wood, coal, lignin, coconut shells, and sugar [7]. The oak plant is of natural carbonaceous material that is used for the preparation of activated carbon. The carbonyl, carboxyl, lactone, phenol, and quinone functional groups on the surface of activated carbon are responsible for their unique adsorption capabilities. The existence of atoms such as nitrogen, oxygen, and sulfur is contingent upon the precursors and activation mechanism employed [8]. Activated carbon is typically produced through a variety of physical and chemical processes. Chemical activation is typically applied to cellulose-containing biomass raw materials, such as wood and fruit pits. Chemical activation involves impregnating the raw material with oxidizing and severely dehydrating chemicals. Subsequently, the suspended material is dried and heated for an adequate time at temperatures varying from 400°C to 900°C. Finally, the produced activated carbon is repeatedly washed to reach a neutral pH [9]. Generally, the shaking technique was used for the uptake of pollutants from water including sodium naproxen and sometimes assisted with ultrasounds. Adsorption onto activated carbon can be enhanced with the use of ultrasonic, which has recently emerged as a promising approach. Cavitation bubbles and localized pressure variations are created within the adsorbent when ultrasonic waves are applied. The targeted pollutants were able to diffuse and mass transfer will be enhanced. The physicochemical parameters of the activated carbon surface can also be adjusted with ultrasonic assistance. It might promote the growth of new active sites or improve the accessibility of existing sites, resulting in increased adsorption capacity. Furthermore, ultrasonic waves can change the pore structure of activated carbon by generating new micropores or broadening existing ones, increasing the surface area accessible for adsorption [10].

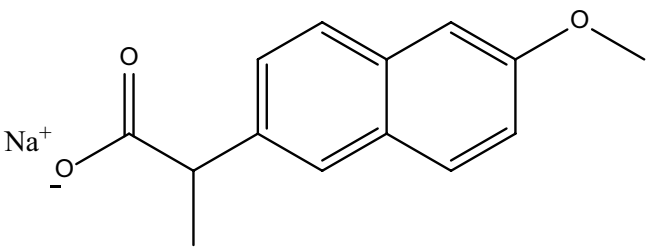

Fig. 1. Sodium naproxen $C_{14}H_{13}NaO_3$.

This research is aimed to investigate the efficacy of using totally ultrasonic for the uptake of sodium naproxen from an aqueous solution and fabricated samples by oak-activated carbon. Parameters of adsorbent dose, starting dye concentration, sonicating time, and pH, were investigated for their efficacy. Kinetic and isothermal studies were conducted to investigate the equilibrium and mechanism of the uptake process.

2. Materials and methods

2.1. Reagents and instruments

Sodium naproxen (Fig. 1), sodium hydroxide 95% purity, and hydrochloric acid 36% were obtained from Sigma-Aldrich (USA) and utilized without further processing. The worker concentrations (10–100 mg·L^{-1}) were prepared from sodium naproxen (SN) stock solutions by dilution. A RANSON 5800, USA ultrasonic water bath was used to accomplish batch adsorption experiments. Fourier-transform infrared spectroscopy (FT-IR; TENSOR from BRUKER, Germany) was utilized to identify functional groups on activated carbon surfaces and their consequences on adsorption. A Zeiss LEO 1550 high-resolution field-emission scanning electron microscopy (FE-SEM, Germany) was implemented to take images of the adsorbent surface. X-ray diffraction patterns were obtained from an XRD D5005 diffractometer (Siemens, Munich, Germany).

2.2. Adsorbent preparation and characterization

Oak fruit was collected from the north of Jordan. Subsequently, the cupules of oak were separated, washed, dried at 80°C for 48 h, ground, impregnated with concentrated phosphoric acid, heated to 450°C, and then washed to neutralization [11]. The prepared oak-based activated carbon (OAC) was subjected to a process of milling and sieving, resulting in the attainment of a particle size of 180 μm. The OAC surface morphology was characterized based on techniques of FT-IR, X-ray diffraction (XRD), and scanning electron microscopy (SEM).

2.2.1. Adsorption experiment

The experimental procedures were carried out exclusively employing an ultrasonic water bath. A solution of SN in various concentrations was combined with a specific amount of OAC and then sonicated for a set amount of time. The lasting quantity of SN was determined based on absorbance measurements. OAC dosage, initial SN concentration, pH, sonication time, and temperature were evaluated for adsorption. A UV-6100 PC double-beam spectrophotometer was employed to examine the concentrations of SN at a wavelength of 237 nm. Eqs. (1) and (2) [12] was employed for the determination of SN amount and percentage of removal by OAC, respectively.

$$q_e = \frac{\left(C_i - C_{\text{eq}}\right)V}{m} \tag{1}$$

$$\%\text{Removal} = \frac{\left(C_i - C_{\text{eq}}\right)}{C_{\text{eq}}} \times 100 \tag{2}$$

where q_e articulate the adsorbed amount of SN in mg·g^{-1}, C_i articulate the initial concentration of SN in mg·L^{-1}, C_{eq} articulate the equilibrium concentration of SN in mg·L^{-1}, V articulate the volume of solution in L, and finally, m is OAC mass in g.

3. Results and discussion

3.1. Characterization of adsorbent

3.1.1. Fourier-transform infrared spectroscopy

FT-IR analysis results demonstrated the existence of multiple functional groups onto both OAC adsorbent and OAC-SN (OAC coated with sodium naproxen after the process of adsorption). Table 1 demonstrates the FT-IR analysis [13]. As a result, noticeable changes in absorbance and intensity confirm SN adsorption onto OAC such as the shift that is remarkable for the hydroxyl group stretching from 3,323.28 to 3,192.10 cm^{-1}, and for the carbonyl group starching from 1,607.06 to 1,798.52 cm^{-1}.

3.1.2. Scanning electron microscopy

The accumulation of SN molecules in aggregates onto the surface of the OAC adsorbent to form the OAC-SN combination (Fig. 2b) compared to the OAC surface (Fig. 2a) confirms the occurrence of the adsorption process. Also, change in the surface porosity and appearance provide additional evidence for the adsorption experience.

3.1.3. XRD analysis of adsorbent material

The XRD analysis presented in Fig. 3 provides compelling evidence for the binding of SN onto OAC. By juxtaposing the XRD profiles of OAC-SN (post-adsorption) with that of OAC (pre-adsorption), it becomes apparent that new peaks, altered peak intensities, and peak broadening confirm the successful accrual of SN onto the OAC substrate.

3.2. Batch adsorption

3.2.1. Comparison study

For comparative purposes, two batch adsorption experiments were conducted under identical conditions (50 mg·L^{-1} initial concentration, pH of 7, 25°C, and contact time of 60 min). Both the first and second experiments were performed in a shaker and an ultrasonic water bath, respectively. Results showed that 88% of SN was adsorbed by sonicating compared to 79% by shaking, demonstrating the superiority of ultrasonic SN removal over shaking.

Table 1
Fourier-transform infrared spectroscopy results of OAC and OAC-SN

	OAC (cm^{-1})	OAC-SN (cm^{-1})
O–H stretching vibration	3,323.28	3,192.10
Aliphatic C–H group stretching vibrations of the alkyl groups	2,885.00	2,677.71
C=O stretching vibration of olefins carbonyl groups in conjugated compounds	1,607.06	1,798.52
Hydroxyl (–OH) stretching of the phenol group	1,565.43	1,556.36
Aromatic skeletal stretching vibration	1,505.78	1,133.926
Aromatic C–H bending vibration (out-of-plane)	877.81	894.85
C–C stretching vibrations	459.18	498.19

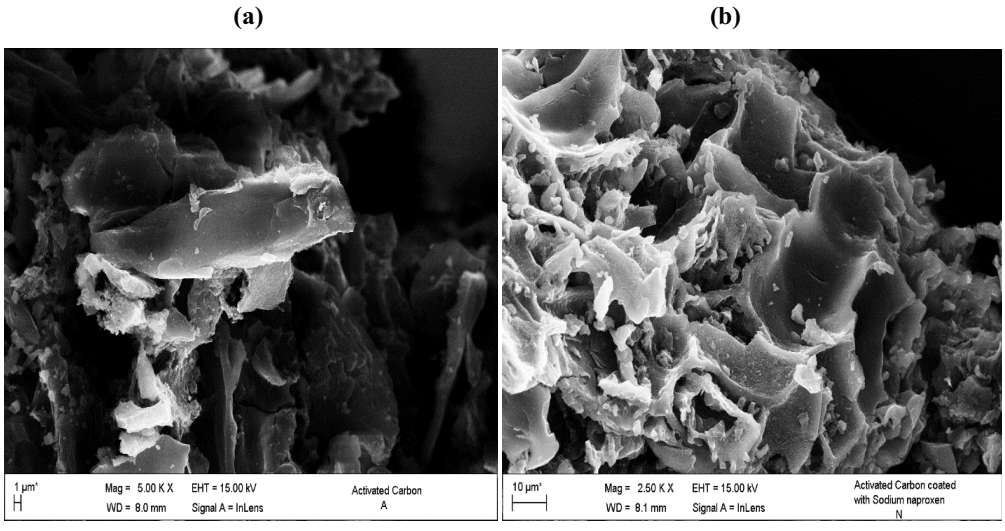

Fig. 2. Scanning electron microscopy analysis of (a) OAC and (b) OAC-SN.

3.2.2. Impact of adsorbent dosage

The uptake percentage is impacted by the dose of the adsorbent. In this study, the dosage of OAC varies from 0.01 to 0.1 g at 25.0°C ± 1°C. Fig. 4 shows the optimal OAC dosage for removing SN, which is found to be 0.06 g. There is a remarkable rise in SN uptake at the beginning due to the accessible adsorption active sights which fall when approaching equilibrium.

3.2.3. Impact of sonication time

This study is based on using sonicating in batch adsorption experiments. When conducting batch adsorption tests, 0.06 g of OAC was sonicated with 50 mg·L^{-1} SN concentration for 15–120 min at 25.0°C ± 1°C. Fig. 5 shows the variation in the uptake of SN by the OAC as time increased. The optimal sonicating time for the uptake of SN by OAC was found to be 60 min.

3.2.4. Impact of SN initial concentration

The impact of initial concentration on the SN uptake by OAC was examined at a concentration range of 10–90 mg·L^{-1} at 25.0°C ± 1°C. Fig. 6 exemplifies the impact of initial concentration on the SN uptake by OAC. The optimal uptake in this experiment was found to be 91.87% by 0.06 g OAC and a concentration of 30.0 mg·L^{-1}. The high uptake of SN at concentrations of 10 and 30 mg·L^{-1} might be attributed to the obtainable sites on the OAC surface. As SN concentration increased, the number of occupied sites on the OAC surface increased, which decreased SN uptake.

3.2.5. Impact of pH

It is important to figure out the pH_{pzc} value, which shows what pH level the surface of the adsorbent is neutral. The pH_{pzc} value was specified by shaking 0.15 g of OAC with 50.0 mL of 0.1 M NaOH solution at a pH value between 2 and 12 for about 24 h. From Fig. 7 it is found that the OAC surface is neutral at pH of 6.58 [14].

In this investigation, a 50 mL of SN solution with a concentration of 50.0 mg·L^{-1} was sonicated with 0.06 g OAC at a temperature of 25°C ± 1°C for 1 h at a pH ranging from 3–11. As shown in Fig. 8, it was discovered that the uptake of SN by OAC increased with decreasing pH values. This result might be attributed to the attraction between the positive OAC surface and the negative SN adsorbate.

3.3. Kinetic and mechanism

Linear and non-linear models including pseudo-first-order, pseudo-second-order, and intraparticle

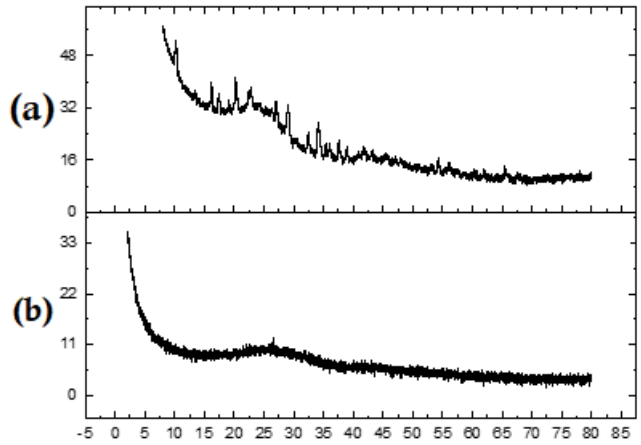

Fig. 3. X-ray diffraction analysis of (a) OAC and (b) OAC-SN.

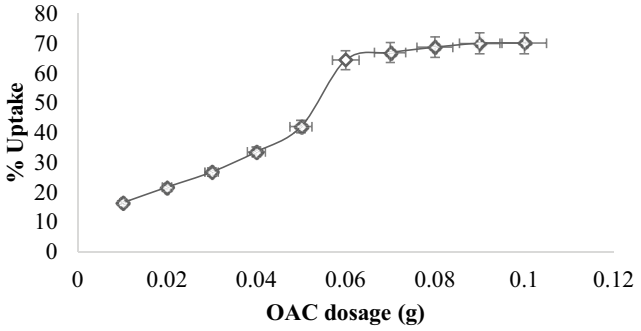

Fig. 4. Impact of OAC dosage on the uptake of SN, (dose = 0.01–0.1 g, C_i = 50 mg·L^{-1}, pH = 7.0, sonicating time = 1.0 h, and T = 25°C ± 1°C).

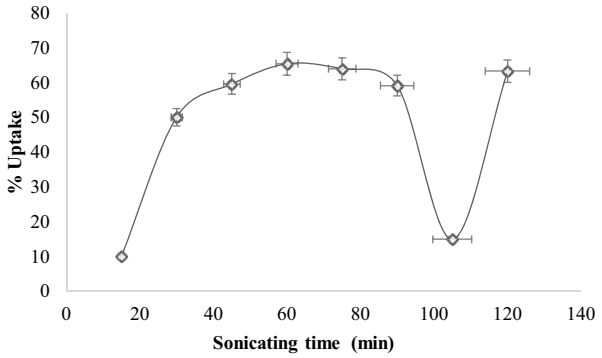

Fig. 5. Impact of sonicating time on SN uptake by OAC, (dose = 0.06 g, C_i = 50 mg·L^{-1}, pH = 7.0, sonicating time = 15–120 min, and T = 25°C ± 1°C).

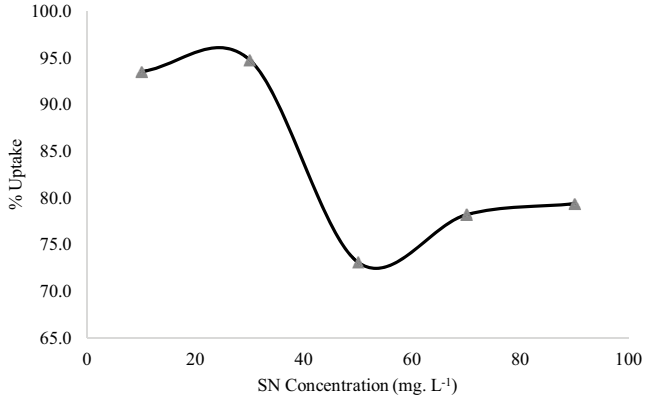

Fig. 6. Impact of initial concentration on the SN uptake by OAC, (dose = 0.06 g, C_i = 10–90 mg·L^{-1}, pH = 7.0, sonicating time = 1.0 h, and T = 25°C ± 1°C).

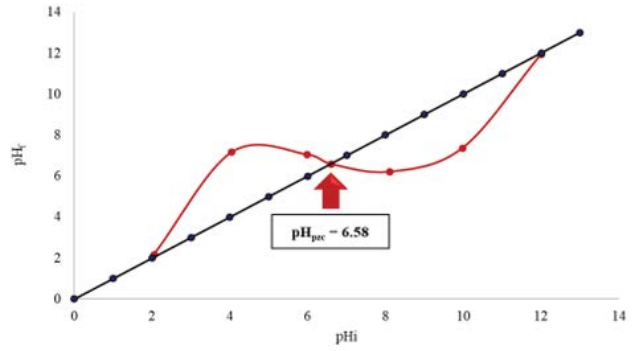

Fig. 7. pH_{pzc} for OAC.

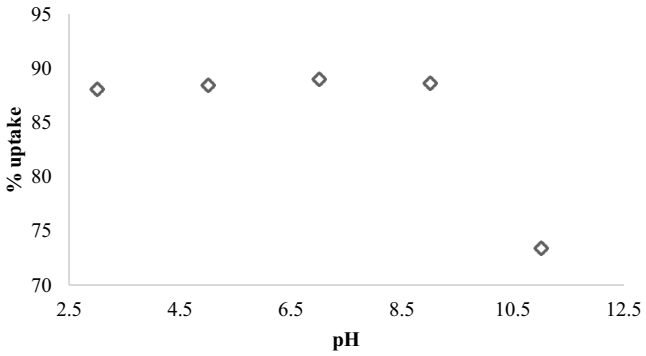

Fig. 8. Impact of pH on the SN uptake by OAC, (dose = 0.06 g, C_i = 50 mg·L^{-1}, pH = 3–11, sonicating time = 1.0 h, and T = 25°C ± 1°C).

diffusion were employed to investigate the kinetics of SN uptake by OAC. Eqs. (3)–(6) [15] were employed to indicate the order of the SN uptake process by OAC. Based on the results shown in Fig. 9, it is unequivocally evident that the pseudo-second-order model provides the best fit for describing the kinetics of SN uptake by OAC. The observed R^2 value of 0.9957 and the estimated rate constant (k_1) of 0.0218 g·mg^{-1}·min^{-1} further confirm the validity and accuracy of the proposed model.

$$\log\left(q_e - q_t\right) = \log\left(q_e\right) - \left(\frac{k_1}{2.303}\right)t \tag{3}$$

$$q_t = q_e\left(1 - e^{-k_1 t}\right)t \tag{4}$$

$$\frac{t}{q_t} = \frac{1}{k_2 q_e^2} - \frac{1}{q_e}t \tag{5}$$

$$q_t = \frac{q_e^2 k_2 t}{q_e k_2 t + 1} \tag{6}$$

where q_e is the amount of SN per unit mass of OAC (mg·g^{-1}) at equilibrium, q_t is the amount of SN per unit mass of OAC at time t (mg·g^{-1}) at equilibrium, and k_1, k_2 are the rate constant in min^{-1} and g·mg^{-1}·min^{-1}, respectively.

The mechanism of the uptake of SN by OAC was indicated by employing the intraparticle diffusion which is exemplified by Eqs. (7) and (8) [16]:

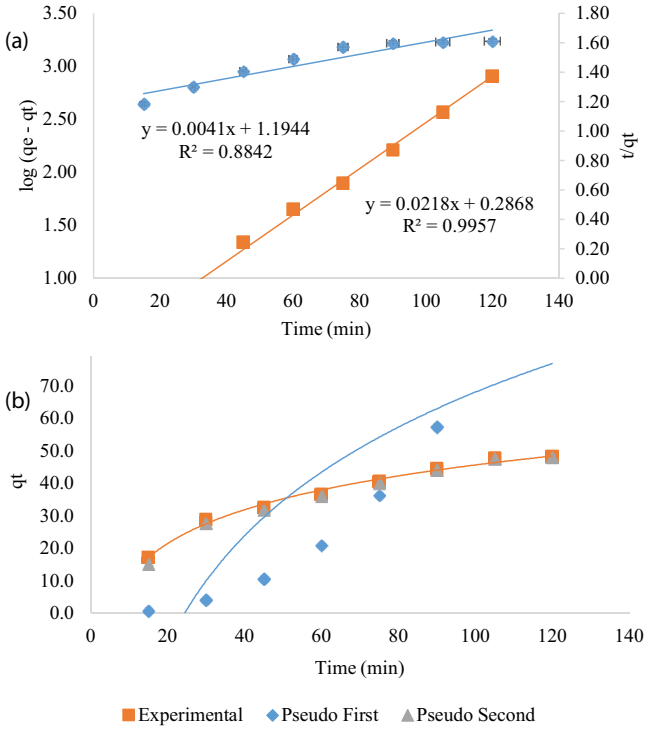

Fig. 9. (a) Linear and (b) non-linear kinetic studies of the SN uptake by OAC, (dose = 0.06 g, C_i = 50 mg·L^{-1}, pH = 7, sonicating time = 10–120 min, and T = 25°C ± 1°C).

$$q_t = K_{id}t^{1/2} + C \tag{7}$$

$$q_t = K_{id}t^{1/2} \tag{8}$$

where q_t is the SN amount (mg·g^{-1}), K_{id} is the rate constant (mg·g^{-1}·min$^{-0.5}$), and $t^{1/2}$ is the square root of time (min$^{0.5}$). Based on the intraparticle diffusion model, it is estimated that if the intercept C = 0, then the intraparticle diffusion would be the only rate-limiting step. When the constant C > 0, then the effect of surface adsorption rises in significance. Fig. 10 shows strong evidence for the hypothesis that the rate-limiting stage in the adsorption process is the surface adsorption step, rather than intraparticle diffusion.

The values of R^2 and constants for all kinetics models are summarized in Table 2.

3.4. Adsorption isotherms

Langmuir [Eqs. (9) and (10)], Freundlich [Eqs. (11) and (12)], Dubinin–Radushkevich [Eqs. (13) and (14)], and Temkin [Eqs. (15) and (16)] isothermal models were employed to elucidate the adsorption mechanism of SN onto OAC [17].

$$\frac{C_e}{q_e} = \frac{1}{k_L q_m} + \frac{C_e}{q_m} \tag{9}$$

$$q_e = \frac{k_L q_m C_e}{\left(1 + k_L C_e\right)} \tag{10}$$

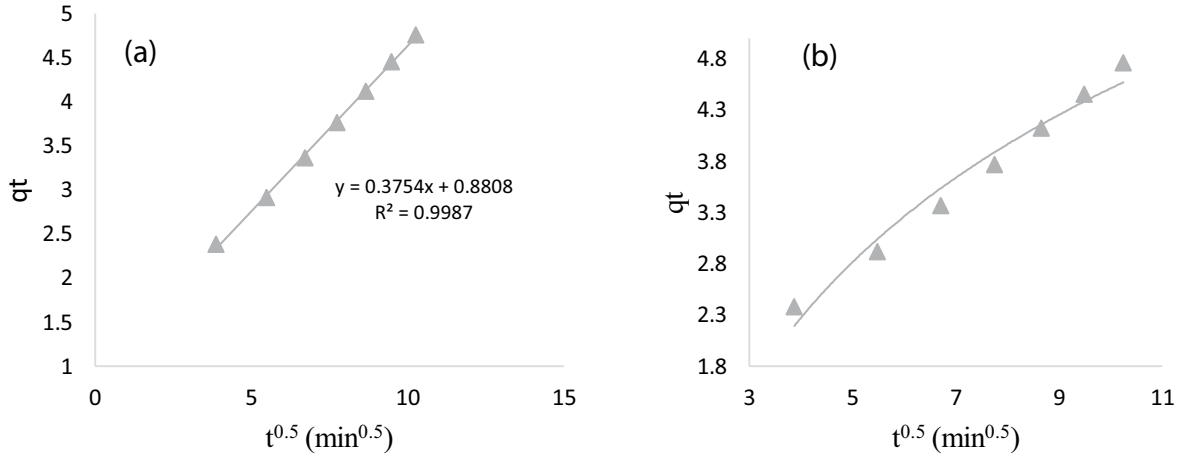

Fig. 10: (a) Linear and (b) non-linear intraparticle model for SN uptake by OAC.

Table 2
Results of kinetics studies for the SN uptake by OAC

		Linear models
Kinetic model	R^2	Related constants
Pseudo-first-order	0.8842	$k_1 = 4.1 \times 10^{-3}$ (min^{-1})
Pseudo-second-order	0.9957	$k_2 = 2.18 \times 10^{-2}$ (g·mg^{-1}·min^{-1})
Intraparticle diffusion	0.8842	$K_{id} = 0.3754$ (mg·g^{-1}·min$^{-0.5}$)

where q_e is the equilibrium quantity of the adsorbate (mg·g^{-1}), C_e is the equilibrium concentration of the adsorbate (mg·L^{-1}), k_L, the constant of Langmuir isotherm that usually employed to determine adsorbate correspondence to the adsorbent surface, q_m is the adsorption capacity (mg·g^{-1}).

$$\log q_e = \log K_f + \frac{1}{n}\log C_e \tag{11}$$

$$q_e = K_F C_e^{1/n} \tag{12}$$

where K_F is the constant of Freundlich isotherm (mg·g^{-1}), and n is the intensity of the adsorption.

$$q_e = B\ln A + B\ln C_e \tag{13}$$

$$q_e = B\ln AC_e \tag{14}$$

where A is the binding constant in g^{-1} at equilibrium, and B is constantly associated with the adsorption heat.

$$\ln q_e = \ln Q_D - B_D\varepsilon^2 \tag{15}$$

$$q_e = q_m e^{-B_D\varepsilon^2} \tag{16}$$

where Q_D is the maximum theoretical capacity (mol·g^{-1}) and B_D is the Dubinin–Radushkevich constant (mol^2·kJ^{-2}). ε (Polanyi potential) in Dubinin–Radushkevich isotherm and the mean energy of the adsorption (kJ·mol^{-1}) could be obtained using Eqs. (17) and (18), respectively.

$$\varepsilon = RT\ln\left(1+\frac{1}{C_e}\right) \tag{17}$$

$$E = \frac{1}{\sqrt{2B_D}} \tag{18}$$

Fig. 11a–d show the results of the linear form of the four isotherms. Correlation coefficients (R^2), dimensional factors, and associated constants were determined based on plots and are summarized in Table 3. The SN uptake by OAC was adequately characterized by the Freundlich isotherm, as indicated by the high R^2 value (0.9953), which indicates multilayer adsorption on heterogeneous sites. The energy value was found to be 9.4 kJ·mol^{-1} (more than 8.0 kJ·mol^{-1}) based on Dubinin–Radushkevich isotherm calculations which indicate a chemical uptake of SN by OAC. The positive value of Temkin constant, B (Table 3), tells that the SN uptake by OAC is exothermic [18].

Fig. 12 shows the results of the non-linear form of the isotherms of Langmuir, Freundlich, and Temkin comparing to the experimental.

3.5. Thermodynamics

Thermodynamic experiments were conducted under optimal conditions at 25°C ± 1°C, 35°C ± 1°C, and 45°C ± 1°C with 1.0 h of sonication. Thermodynamic considerations $\Delta G°$, $\Delta H°$, and $\Delta S°$ were calculated to estimate the efficacy of SN uptake by OAC (Table 4). The SN uptake enthalpy change $\Delta H°$ (kJ·mol^{-1}) and entropy change $\Delta S°$ (J·mol^{-1}·K^{-1}) change were calculated from the slope and intercept of the plot of ln(k_L) vs. 1/T (K^{-1}) Eq. (19), respectively. Free Gibbs Energy, $\Delta G°$, was calculated based on Eq. (20).

$$\ln\left(K_L\right) = \frac{\Delta S°}{R} - \frac{\Delta H°}{T}\left(\frac{1}{T}\right) \tag{19}$$

$$\Delta G° = -RT\ln\left(K_L\right) \tag{20}$$

where K_L is dimensionless and corresponds to the adsorption equilibrium constant according to the best-fitted model,

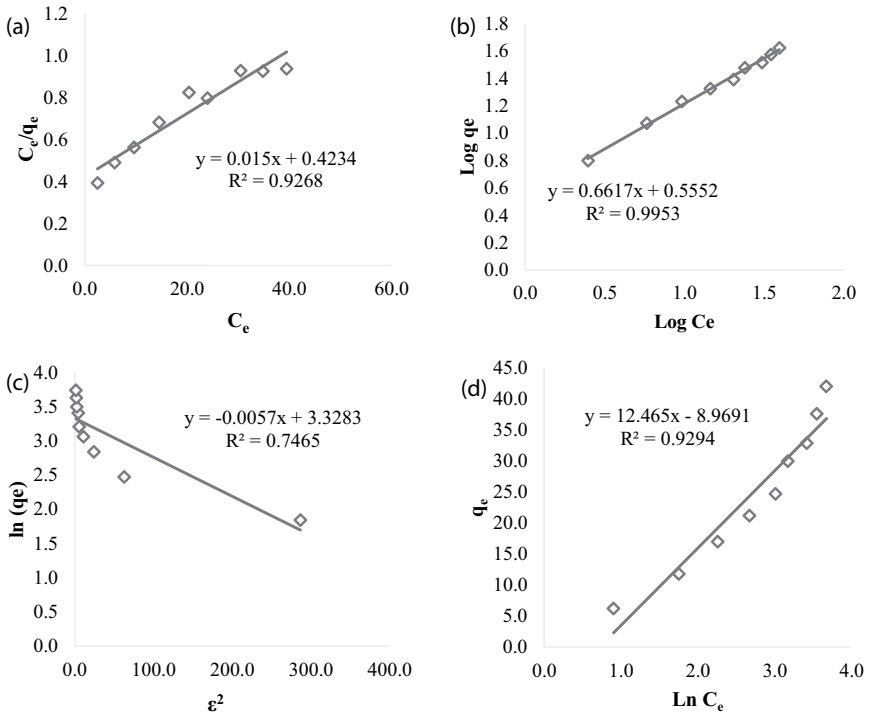

Fig. 11. Linear isotherms of (a) Langmuir, (b) Freundlich, (c) Temkin, and (d) Dubinin–Radushkevich of SN uptake by OAC.

Table 3
Isotherms model constants

Isotherm	Related isotherms constants	
Langmuir	R_L^2	0.9268
	K_L	0.035
	q_m, mg·g^{-1}	94.8
Freundlich	R_F^2	0.9953
	K_F, mg·g^{-1}	1.74
	n	1.5
Dubinin–Radushkevich	R^2	0.7465
	B_D, mol^2·kJ^{-2}	5.7 × 10^{-3}
	E, kJ·mol^{-1}	9.4
Temkin	R^2	0.9294
	B	12.47
	A	0.1909

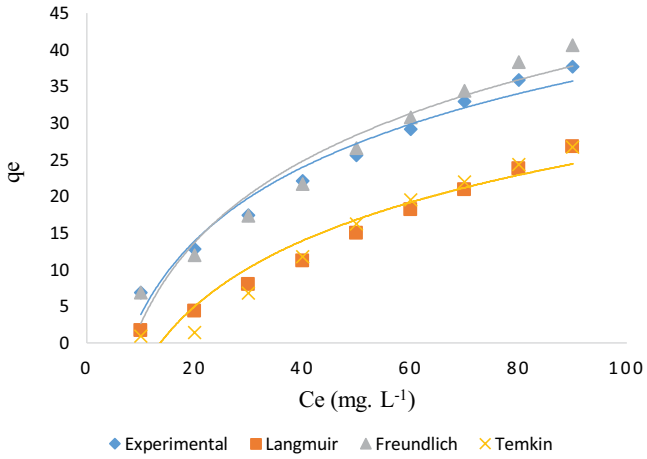

Fig. 12. Non-linear isotherms of (a) Langmuir, (b) Freundlich, and (c) Temkin of SN uptake by OAC.

Table 4
Thermodynamic parameters of SN uptake by OAC

Adsorbent	T (K)	q_m (mg·g^{-1})	Thermodynamic parameters		
			$\Delta G°$ (kJ·mol^{-1})	$\Delta H°$ (kJ·mol^{-1})	$\Delta S°$ (kJ·K^{-1}·mol^{-1})
OAC	298	80.65	11.81	10.88	–3.16
	308	77.45	11.85		
	318	62.13	11.88		

R is the universal constant of ideal gases, 8.314 J·K^{-1}·mol^{-1}. The +ve obtained value of $\Delta G°$ (11.81, 11.85, and 11.88 kJ·mol^{-1}) implies the non-spontaneity of the SN uptake by OAC. The +ve obtained value of $\Delta H°$ (10.88 kJ·mol^{-1}) implies the endothermic nature of the SN uptake by OAC and a physisorption through van der Waals (less than 20 kJ·mol^{-1}) [19]. The –ve value of $\Delta S°$ implies adsorbate/adsorbent interface irregularity and adsorbent affinity [20].

3.6. Fabricated sample

A tablet of three commercial SN medications was dissolved in tap water and sonicated with 50 mg OAC for

60.0 min under optimum conditions. The SN uptake was found to be 85.27%, 81.25%, and 78.12% (Fig. 13), proving the efficacy of OAC in the uptake of SN by sonication.

4. Comparison with other activated carbon adsorbents

Other activated carbon adsorbents based on the shaking process were compared to OAC's maximal SN uptake capabilities (Table 5). According to the comparison, OAC has an adsorption capacity of 94.8 mg·g^{-1}, which is comparable to several other known adsorbents.

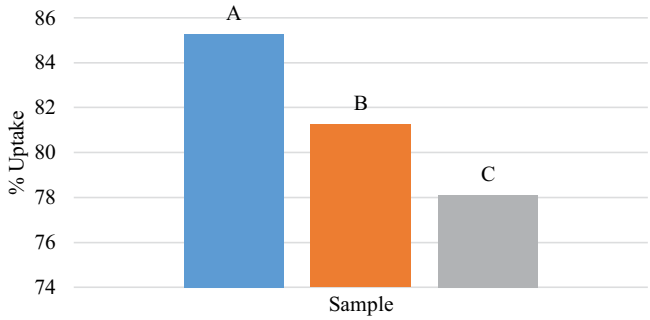

Fig. 13. Uptake of SN by OAC for fabricated samples.

Table 5
Comparison of SN uptake by OAC with other reported adsorbents

Adsorbent	q_{max} (mg·g^{-1})	References
Waste apricot AC	106.38	[12]
Peanut shells AC	105	[21]
Olive-waste cake AC	95.7	[22]
Spent coffee wastes AC	61.0	[23]
Jaboticaba peels AC	167	[24]
Grape residues AC	176	[24]
Pitaya peels AC	158.81	[24]
Oak cupule AC	94.8	(Present study)

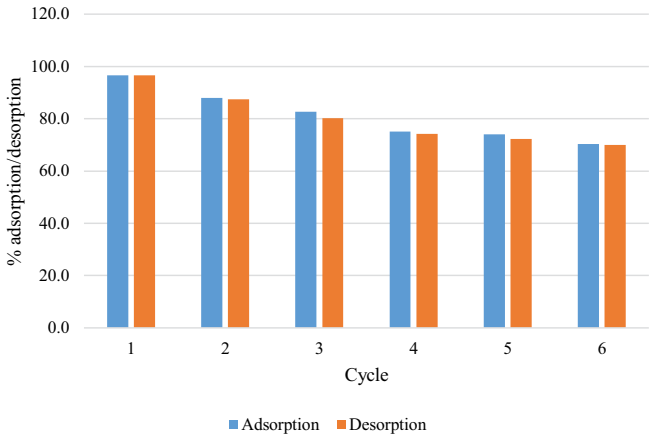

Fig. 14. Regeneration of OAC adsorbent.

5. Regeneration of OAC

Based on the impact of the pH experiment, it's been found that sodium hydroxide is suitable choice for the regeneration investigation. SN was eluted from OAC using 1.0 M NaOH. The percentage of desorption was calculated using Eq. (21) [25,26].

$$\%\text{Desorption} = \frac{C_{de}}{C_{ad}} \times 100 \tag{21}$$

whereas C_{de} is SN desorbed concentration and C_{ad} is the SN adsorbed concentration. Fig. 14 shows that after six cycles, the uptake of SN declined from 96.68% to 70.25%, indicating the capability of OAC to be reused about 24 times.

6. Conclusion

The present study demonstrates the efficient uptake of SN from aqueous solutions and fabricated samples by the utilization of activated carbon obtained from oak cupule (OAC) via ultrasonic treatment. Using ultrasonic waves to enhance the adsorption process offers several advantages, including enhanced mass transfer, disruption of diffusion layers, and the potential for synergistic effects. The experimental results have conclusively determined the optimal conditions that are best suited for achieving maximum uptake of SN by OAC. Based on the experimental data, it has been unequivocally determined that the optimal conditions for SN uptake by OAC entail a 60-min sonication period, 0.06 g of OAC, a pH of 7.0, and a concentration of 30 mg·L^{-1}. The maximum uptake of SN was found to be a remarkable 94.80% under these conditions. The kinetics and isothermal studies conducted in this research have demonstrated that the uptake of SN by OAC conforms well to the pseudo-second-order kinetic model and the Freundlich isothermal model. Furthermore, the thermodynamic analysis revealed that the process of SN uptake by OAC is endothermic and non-spontaneous. After six cycles, OAC's effectiveness would fall by 26.43%, but it would still be functioning.

Ethical approval

We confirm that this work is original and has not been published elsewhere nor is it currently under consideration for publication elsewhere.

Author contributions

"All authors contributed to the study conception and design. Material preparation, data collection, and analysis were performed by all authors. The first draft of the manuscript was written by Alaa Mahmoud Al-Ma'abreh and all authors commented on previous versions of the manuscript. All authors read and approved the final manuscript".

Funding

"This research was funded by Isra University with grant number of [8-38/2020/2021]".

Competing interests

The authors declare that they have no conflict of interest.

Availability of data and materials

The data that support the findings of this study are available within the article.

References

[1] A. Nikolaou, S. Meric, D. Fatta, Occurrence patterns of pharmaceuticals in water and wastewater environments, Anal. Bioanal. Chem., 387 (2007) 1225–1234.

[2] A.L. Moreno Ríos, K. Gutierrez-Suarez, Z. Carmona, C.G. Ramos, L.F.S. Oliveira, Pharmaceuticals as emerging pollutants: case naproxen an overview, Chemosphere, 291 (2022) 132822, doi: 10.1016/j.chemosphere.2021.132822.

[3] A. Saravanan, P. Senthil Kumar, S. Jeevanantham, S. Karishma, B. Tajsabreen, P.R. Yaashikaa, B. Reshma, Effective water/wastewater treatment methodologies for toxic pollutants removal: processes and applications towards sustainable development, Chemosphere, 280 (2021) 130595, doi: 10.1016/j.chemosphere.2021.130595.

[4] M.A. Khan, Sh.M. Wabaidur, M.R. Siddiqui, A.A. Alqadami, A.H. Khan, Silico-manganese fumes waste encapsulated cryogenic alginate beads for aqueous environment de-colorization, J. Cleaner Prod., 240 (2020) 118867, doi: 10.1016/j.jclepro.2019.118867.

[5] S. Babel, T.A. Kurniawan, Low-cost adsorbents for heavy metals uptake from contaminated water: a review, J. Hazard. Mater., 97 (2003) 219–243.

[6] C. Jung, A. Son, N. Her, K.-D. Zoh, J. Cho, Y. Yoon, Removal of endocrine disrupting compounds, pharmaceuticals, and personal care products in water using carbon nanotubes: a review, J. Ind. Eng. Chem., 27 (2015) 1–11.

[7] Ç. Sarıcı-Özdemir, Y. Önal, S. Erdoğan, C. Akmil-Başar, Studies on removal of naproxen sodium by adsorption onto acf in batch and column, Fresenius Environ. Bull., 21 (2012) 84–93.

[8] Z. Heidarinejad, M.H. Dehghani, M. Heidari, G. Javedan, I. Ali, M. Sillanpää, Methods for preparation and activation of activated carbon: a review, Environ. Chem. Lett., 18 (2020) 393–415.

[9] M.A. Yahya, Z. Al-Qodah, C.W. Zanariah Ngah, Agricultural bio-waste materials as potential sustainable precursors used for activated carbon production: a review, Renewable Sustainable Energy Rev., 46 (2015) 218–235.

[10] Y. Yao, Enhancement of mass transfer by ultrasound: application to adsorbent regeneration and food drying/dehydration, Ultrason. Sonochem., 31 (2016) 512–531.

[11] M. Alkhabbas, A.M. Al-Ma'abreh, G. Edris, T. Saleh, H. Alhmood, Adsorption of anionic and cationic dyes on activated carbon prepared from oak cupules: kinetics and thermodynamics studies, Int. J. Environ. Res. Public Health, 20 (2023) 3280, doi: 10.3390/ijerph20043280.

[12] Y. Onal, C. Akmil-Başar, C. Sarici-Ozdemir, Elucidation of the naproxen sodium adsorption onto activated carbon prepared from waste apricot: kinetic, equilibrium and thermodynamic characterization, J. Hazard. Mater., 148 (2003) 727–734.

[13] J. Bedia, M. Peñas-Garzón, A. Gómez-Avilés, J.J. Rodriguez, C. Belver, A review on the synthesis and characterization of biomass-derived carbons for adsorption of emerging contaminants from water, J. Carbon Res., 4 (2018) 63, doi: 10.3390/c4040063.

[14] Y. Sun, H. Li, G. Li, B. Gao, Q. Yue, X. Li, Characterization and ciprofloxacin adsorption properties of activated carbons prepared from biomass wastes by H_3PO_4 activation, Bioresour. Technol., 217 (2016) 239–244.

[15] N.S. Kumar, M. Asif, M.I. Al-Hazzaa, Adsorptive removal of phenolic compounds from aqueous solutions using pine cone biomass: kinetics and equilibrium studies, Environ. Sci. Pollut. Res., 24 (2018) 21949–21960.

[16] R. Lafi, I. Montasser, A. Hafiane, Adsorption of congo red dye from aqueous solutions by prepared activated carbon with oxygen-containing functional groups and its regeneration, Adsorpt. Sci. Technol., 37 (2018) 160–181.

[17] A.M. Al-Ma'abreh, R.A. Abuassaf, D.A. Hmedat, M. Alkhabbas, G. Edris, S.H. Hussein-Al-Ali, S. Alawaideh, Adsorption characteristics of hair dyes removal from aqueous solution onto oak cupules powder coated with ZnO, Int. J. Mol. Sci., 23 (2022) 11959, doi: 10.3390/ijms231911959.

[18] E. Malkoc, Y. Nuhoglu, Fixed bed studies for the sorption of chromium(VI) onto tea factory waste, Chem. Eng. Sci., 61 (2006) 4363–4372.

[19] G.R. Mahdavinia, F. Bazmizeynabad, B. Seyyedi, *Kappa*-carrageenan beads as new adsorbent to remove crystal violet dye from water: adsorption kinetics and isotherm, Desal. Water Treat., 53 (2015) 2529–2539.

[20] Q. Li, Q.-Y. Yue, Y. Su, B.-Y. Gao, H.-J. Sun, Equilibrium, thermodynamics and process design to minimize adsorbent amount for the adsorption of acid dyes onto cationic polymer-loaded bentonite, Chem. Eng. J., 158 (2010) 489–497.

[21] F. Tomul, Y. Arslan, B. Kabak, D. Trak, E. Kendüzler, E.C. Lima, H.N. Tran, Peanut shells-derived biochars prepared from different carbonization processes: comparison of characterization, Sci. Total Environ., 726 (2020) 137828, doi: 10.1016/j.scitotenv.2020.137828.

[22] R. Baccar, M. Sarrà, J. Bouzid, M. Feki, P. Blánquez, Removal of pharmaceutical compounds by activated carbon prepared from agricultural by-product, Chem. Eng. J., 211 (2012) 310–317.

[23] J. Shin, J. Kwak, Y.-G. Lee, S. Kim, M. Choi, S. Bae, S.-H. Lee, Y. Park, K. Chon, Competitive adsorption of pharmaceuticals in lake water and wastewater effluent by pristine and NaOH-activated biochars from spent coffee wastes: contribution of hydrophobic and π-π interactions, Environ. Pollut., 270 (2021) 116244, doi: 10.1016/j.envpol.2020.116244.

[24] D.S.P. Franco, J. Georgin, M.S. Netto, K. da Boit Martinello, L.F.O. Silva, Preparation of activated carbons from fruit residues for the removal of naproxen (NPX): analytical interpretation via statistical physical model, J. Mol. Liq., 356 (2022) 119021, doi: 10.1016/j.molliq.2022.119021.

[25] P.V. Nidheesh, R. Gandhimathi, S.T. Ramesh, T.S. Anantha Singh, Adsorption and desorption characteristics of crystal violet in bottom ash column, J. Urban Environ. Eng., 6 (2012) 18–29.

[26] A.M. Al-Ma'abreh, R.A. Abuassaf, D.A. Hmedat, M. AlKhabbas, S. Alawaideh, G. Edris, Comparative study for the removal of crystal violet from aqueous solution by natural biomass adsorbents of a pinecone, cypress, and oak: kinetics, thermodynamics, and isotherms, Desal. Water Treat., 274 (2022) 245–260.